Linc00961 inhibits the proliferation and invasion of skin melanoma by targeting the miR-367/PTEN axis

XIN MU, KUAN-HOU MOU, RUI GE, DAN HAN, YAN ZHOU and LI-JUAN WANG

Department of Dermatology, First Affiliated Hospital of Xi'an Jiaotong University, Xi'an, Shaanxi 710061, P.R. China

Abstract. Long intergenic noncoding RNA 00961 (Linc00961) has been identified as a tumor suppressor in various types of cancer. However, the critical roles of Linc00961 in the carcinogenesis and progression of skin melanoma (SM) are yet to be fully elucidated. The present study revealed via reverse transcription-quantitative PCR analysis that Linc00961 was downregulated in the tissues of patients with SM compared with benign nevi, and in A375, A2058 and SK-MEL-28 cell lines compared with human melanocytes. Furthermore, overexpression of Linc00961 inhibited cell proliferation, and promoted the apoptosis of A375 and SK-MEL-28 cells *in vitro* and *in vivo*, as determined by Cell Counting Kit-8 and flow cytometry assays, and tumor xenograft studies, respectively. Overexpression of Linc00961 also led to an attenuation of the migration and invasive capabilities of A375 and SK-MEL-28 cells, measured using Transwell assays. Functionally, it was demonstrated that Linc00961 acted as a competing endogenous RNA (ceRNA) by competitively sponging microRNA-367 (miR-367) in A375 and SK-MEL-28 cells; restoration of miR-367 rescued the inhibitory effects of Linc00961 on A375 and SK-MEL-28 cells. Finally, it was observed that phosphate and tension homology deleted on chromosome 10 (PTEN), an established target of miR-367 in A375 and SK-MEL-28 cells, was positively regulated by Linc00961, and its inhibition reversed the inhibitory effects of Linc00961 on the proliferation and invasion of A375 and SK-MEL-28 cells. Collectively, the present study revealed that Linc00961 was downregulated in SM, and furthermore, Linc00961 was identified as a ceRNA that inhibits the proliferation and invasion of A375 and SK-MEL-28 cells by modulating the miR-367/PTEN axis.

Introduction

At present, skin melanoma (SM) remains the most frequently occurring and aggressive type of cutaneous cancer, and it is estimated that, in addition to the markedly increased incidence of SM over the course of the last decade, there will be 96,480 newly diagnosed cases of SM in the USA in 2019 (1). Despite the continuing improvements that have been made in terms of diagnosis and treatment, the recommended maintenance schedules, from radical resection to molecular-targeted drugs, at present are only effective in a subset of patients (2,3). The tumors are often found to have metastasized to distant sites or visceral organs in patients even at an early stage of diagnosis, and the 5-year overall survival rate remains extremely disappointing for this subset of patients, with a median survival time of 6-9 months (4). Therefore, in order to establish novel treatment therapies for SM, it is important to explore in detail the underlying molecular mechanisms and identify novel molecules to counteract the progression of SM.

Long non-coding RNAs (lncRNAs) are a class of non-protein-coding transcripts (>200 nucleotides in length) that have been reported to serve pivotal roles in physiological and pathophysiological processes associated with the reproductive, metabolic, endocrine, cardiovascular and nervous systems (5-7). Of greater importance considering the present study, lncRNAs have been also identified as crucial regulators in the carcinogenesis and progression of multiple types of cancer, where they function as oncogenes or tumor suppressors, depending on the cancer type and the prevailing circumstances (8-10). In the case of SM, an increasing body of evidence has indicated that lncRNAs are also involved in the regulation of the expression and function of established oncogenes or tumor suppressors, either post-transcriptionally or via chromatin regulation (11-13). Nevertheless, only a small number of lncRNAs have been functionally characterized at present, and the mechanisms underlying their biological functions are yet to be fully elucidated.

Long intergenic noncoding RNA 00961 (Linc00961), located in chromosome 9 and 1,546 nucleotides in length, was reported to be an encoder of small regulatory polypeptide of amino acid response (SPAAR), and is involved in muscle

Correspondence to: Dr Li-Juan Wang, Department of Dermatology, First Affiliated Hospital of Xi'an Jiaotong University, 227 Yanta West Road, Xi'an, Shaanxi 710061, P.R. China
E-mail: 6945216juan@163.com

Abbreviations: SM, skin melanoma; BN, benign nevi; lncRNA, long noncoding RNA; Linc00961, long intergenic noncoding RNA 00961; miR-367, microRNA-367; PTEN, phosphate and tension homology deleted on chromosome 10; SPAAR, small regulatory polypeptide of amino acid response; NSCLC, non-small cell lung cancer; FISH, fluorescent *in situ* hybridization

regeneration (14,15). Furthermore, recent studies have also identified Linc00961 as a tumor suppressor in multiple types of cancers, including glioma (16) and non-small cell lung cancer (NSCLC) (17). However, the expression profile, biological function and clinical significance of Linc00961 have not been fully investigated.

The aims of the present study were to identify the expression and function of Linc00961 in SM. It was revealed that Linc00961 was downregulated in SM, and functioned as a competitive endogenous RNA (ceRNA) to positively regulate the expression of phosphate and tension homology deleted on chromosome 10 (PTEN) by sponging microRNA (miRNA/miR)-367 in A375 and SL-MEL-28 cells. Collectively, these results demonstrated the tumor suppressor role of Linc00961 in the carcinogenesis and progression of SM.

Materials and methods

Clinical specimens. The present study was performed in accordance with the principles of the Declaration of Helsinki and approved by the Ethical Committee of the First Affiliated Hospital of Xi'an Jiaotong University. Pathologically diagnosed SM or benign nevi (BN) patients were enrolled in this study. Tissues from a total of 13 patients with SM (aged 34-68 years; 5 male and 8 female) and 13 BN tissues from different cohorts of patients (aged 29-67 years; 5 male and 8 female) were collected at the First Affiliated Hospital of Xi'an Jiaotong University between January 2010 and August 2017. All the patients enrolled in the present study provided their informed consent for the use of their resected tissues in this research.

Cell culture. Human A375 (cat. no. GCC-ME0001CS), SK-MEL-28 (cat. no GCC-ME0003CS) and A2058 (cat. no. GCC-ME0004CS) SM cell lines, and human epidermal HEMa-LP melanocytes (cat. no. GCC-NC0027CS) were all purchased from Shanghai GeneChem Co., Ltd., where they were characterized by mycoplasma detection, isozyme detection and DNA fingerprinting. HEMa-LP cells were cultured in Invitrogen® Medium 254 (Thermo Fisher Scientific, Inc.) supplemented with human melanocyte growth supplement (Thermo Fisher Scientific, Inc.), and A375, A2058, and SK-MEL-28 cells were cultured in Gibco® Dulbecco's Modified Eagle's medium (DMEM; Gibco; Thermo Fisher Scientific, Inc.) supplemented with 10% fetal bovine serum (CellMax) and 100 U/ml penicillin and streptomycin (CellMax) at 37°C in a humidified atmosphere of 5% CO_2.

Bioinformatics analysis. The expression of Linc00961 in the Gene Expression Omnibus (https://www.ncbi.nlm.nih.gov/geo/) dataset (GSM3071633) (18), containing data for 57 patients with SM and 23 patients with BN, was analyzed using the R2: Genomics Analysis and Visualization Platform (http://r2.amc.nl). The associations between Linc00961 expression and the overall survival of patients with SM in The Cancer Genome Atlas (TCGA) database (https://cancergenome.nih.gov/) was analyzed using Gene Expression Profiling Interactive Analysis (http://gepia.cancer-pku.cn). High and low expression were predefined in this cohort prior to the present study. The potential miRNAs containing putative binding sites for Linc00961 were identified using miRDB (version 2.0; http://mirdb.org/).

Reverse transcription-quantitative polymerase chain reaction (RT-qPCR). RNA/miRNA extraction and RT-qPCR were performed as previously described in a study by the present authors (19). In brief, total RNA was extracted form A375, A2058, and SK-MEL-28 cells or the tissues of patients with SM. RNA samples were then reverse transcribed into cDNA (PrimeScript™ RT Reagent kit; Takara Bio, Inc.). Then, SYBR Green Mix (Takara Bio, Inc.) was used to detect and quantify Linc00961, miR-367, β-actin and U6 expression. The thermocycling conditions were as follows: Denaturation at 95°C for 7 min, followed by 35 cycles of 95°C for 5 sec, 60°C for 30 sec, 72°C for 3 min. The relative expression level was calculated using the $2^{-\Delta\Delta Cq}$ method (20). The primers used in this study were purchased from Sangon Biotech Co., Ltd., and their sequences are presented in Table SI.

Lentivirus vector construction and transfection. Lentivirus vector overexpressing Linc00961 (Lv-Linc00961) was designed and constructed by Shanghai GeneChem Co., Ltd. Briefly, the full length of Linc00961 was chemically synthesized and cloned into the *Bam*HI and *Age*I sites of a CV146 lentivirus core vector. Subsequently, CV146-Linc00961 (20 μg) and lentiviral packaging helper plasmids, Helper 1.0 (15 μg) and Helper 2.0 (10 μg; both Shanghai GeneChem Co.,Ltd.), were co-transfected into 293T cells using Lipofectamine™ 2000 (Thermo Fisher Scientific, Inc.). The cell supernatant was collected 48 h later, and subjected to centrifugation (4°C, 4,000 x g, 10 min) in order to concentrate and purify Lv-Linc00961. Cells stably expressing Linc00961 were constructed by transfecting $5x10^5$ TU Lv-Linc00961 or Lv-control (containing empty CV146 vector) into $2x10^6$ A375 or SK-MEL-28 cells cultured in 1 ml enhanced infection solution (Shanghai GeneChem Co., Ltd.). Then, 5 μg polybrene (Shanghai GeneChem Co., Ltd.) was added in each well according to the manufacturer's protocol (17). Transfected cells were harvested 72 h later, and subsequently treated with puromycin (2 μg/ml) in order to isolate the Linc00961-stably-expressing cells.

Small interfering RNA (siRNA) and miRNA transfection. PTEN siRNA (sense, 5'-GAGCGUGCAGAUAAUGACA-3'; antisense, 3'-CUCGCACGUCUAUUACUGU-5'), negative control (NC) siRNA (sense, 5'-UUCUCCGAACGUGUC AGGUTT-3'; antisense, 3'-ACCUGACACGUUCGGAGA ATT-5'), miR-367 mimics (5'-AGUGGUAACGAUUUCACG UUAA-3'), and miR-367 NC (5'-GUGGAUAUUGUUGCC AUCA-3') were purchased from Shanghai GenePharma Co., Ltd. Transfection was performed as previously described (19). Briefly, $1x10^6$ A375 or SK-MEL-28 cells were seeded in 6-well plates, PTEN siRNA (50 nM), normal control siRNA (50 nM), miR-367 mimics (50 nM) or miR-367 NC (50 nM) were mixed with 5 μl Lipofectamine 2000 in 500 μl serum-free DMEM. Then, the solutions were added to each well. The cells were collected at 72 h after transfections for Cell Counting Kit-8 (CCK-8), flow cytometry (FCM) and Transwell assays.

CCK-8, FCM and Transwell assays. A375 and SK-MEL-28 cells were transfected with Lv-Linc00961, Lv-Linc00961 + miR-367 mimics, Lv-Linc00961 + PTEN siRNA and corresponding controls as aforementioned. Then, the proliferation of transfected cells was measured using a CCK-8

assay (MedChemExpress) at 0, 24, 48, 72, 96 and 120 h following transfection, whereas cell apoptosis was measured using an Annexin-V/PI kit (BD Biosciences); the percentage of early apoptotic cells was analyzed using FlowJo 10 software (FlowJo LLC), and cell migration and invasion were measured using Transwell (Corning Inc.) and Matrigel (BD Biosciences) assays at 72 h following transfection. All the procedures for the CCK-8, FCM and Transwell assays were performed as described in our previous study (19).

For the Transwell assays, briefly, A375 and SK-MEL-28 cells were suspended in serum-free DMEM at a density of $4x10^5$ cells/ml. Then, cells (200 μl) were seeded in the upper chamber coated with (for the invasion assay) or without (for the migration assay) Matrigel (BD Biosciences). DMEM with 10% FBS (600 μl) was added to the lower chamber. After the cells had been allowed to migrate for 24 h or to invade for 48 h, the penetrated cells on the filter were fixed in dried methanol for 1 min and stained in 4 g/l crystal violet for 10 min (both at room temperature). The numbers of migrated or invasive cells were determined from five random fields using a light microscope (magnification, x100; Olympus Corporation).

Western blotting. Proteins were extracted from the transfected cells at 72 h after transfection using RIPA buffer (cat. no. P0013B; Beyotime Institute of Biotechnology) and quantified using a bicinchoninic acid protein assay kit (cat. no. P0011; Beyotime Institute of Biotechnology). Then, 20 μg/lane protein from different transfected cells was separated via 10% SDS-PAGE and transferred to PVDF membranes. The PVDF membranes were blocked with 1X Blocker™ BSA in TBS (cat. no. 37520; Thermo Fisher Scientific, Inc.) for 2 h at room temperature. Then, the PVDF membranes were incubated overnight at 4℃ with rabbit-anti-human PTEN (1:400; cat. no. 9188; Cell Signaling Technology, Inc.) and β-actin (1:1,000, cat. no. 4970; Cell Signaling Technology, Inc.) primary antibodies. After incubating with the horseradish peroxidase-conjugated goat anti-rabbit IgG secondary antibodies (1:5,000; cat. no. 7074; Cell Signaling Technology, Inc.) for 2 h at room temperature, the signals were detected using SignalFire™ Plus ECL Reagent (cat. no. 12630; Cell Signaling Technology, Inc.).

Fluorescence in situ hybridization (FISH). Oligonucleotide modified probes for Linc00961 (cat. no. lnc1CM001) and U6 (cat. no. lnc110101) were purchased from Guangzhou RiboBio Co., Ltd. SK-MEL-28 cells ($1x10^6$) were seeded in 18-mm confocal dishes. Following overnight incubation, the cells were fixed with 4% paraformaldehyde for 20 min and permeabilized with Triton X-100 for 90 sec (both at room temperature). Then, SK-MEL-28 cells were incubated with hybridization buffer supplemented with 100 μl Linc00961 and U6 FISH probes (20 μM) at 37℃ overnight in a dark moist chamber. The following day, cells were washed three times in 2X saline-sodium citrate buffer and stained with DAPI for 5 min at room temperature. The images were acquired using a confocal microscope (magnification, x400; Olympus Corporation).

In vivo xenograft experiments. For tumorigenesis assays, xenograft tumors were generated by subcutaneous injection of A375 cells ($5x10^6$) stably expressing Linc00961 or infected with Lv-control into the hind limbs of female Balb/C athymic nude mice (nu/nu; Animal Center of Xi'an Jiaotong University) weighing 18-20 g and aged 6 weeks old (n=3/group). All mice were housed and maintained under specific pathogen-free conditions at 18-22℃, with 20% humidity, a 12 h light:12 h dark cycle, and with commercial rat food and water *ad libitum*. All experiments were approved by the Animal Care and Use Committee of Xi'an Jiaotong University and performed in accordance with institutional guidelines. Tumor size and weight were measured using Vernier calipers and an electronic balance every 7 days. Tumor volume was determined according to the formula: $0.5x AxB^2$, where A represents the diameter of the base of the tumor, and B represents the corresponding perpendicular value. After 35 days, the mice were weighed, and the weights of the mice at 35 days were all between 20-22 g. Then, the mice were anesthetized using isoflurane and sacrificed in a CO_2 chamber for 7 min, where the flow rate displaced no more than 30% chamber volume/min. Once death was confirmed, the tumors were collected and weighed. Symptoms such as pain, weight loss, loss of appetite or weakness were set as humane endpoints for the present study; however, no animal was sacrificed before the completion of the 35-day experiment as a result of displaying any of these symptoms.

TUNEL and Ki-67 staining. The resected xenograft tumors were fixed in 4% paraformaldehyde for 24 h at room temperature. Then, resected tumors were desiccated with ascending series of ethanol, cleared in xylene, dipped in wax, embedded in paraffin and sectioned. Subsequently, tissue sections (5-μm thick) were deparaffinized and rehydrated. For TUNEL staining, the slides were incubated with Proteinase K (20 μg/ml in 10 mM Tris/HCL, pH 7.4) for 30 min at 37℃ and 50 μl TUNEL reaction mixture (Roche Diagnostics) for 60 min at 37℃. Subsequently, the slides were stained with 200 nM DAPI for 5 min at room temperature to visualize the nuclei.

For Ki-67 staining, slides were incubated in citric acid antigen retrieval solution for 100 sec at 110℃ in an autoclave. After washing with PBS for three times, the slides were incubated with 3% H_2O_2 for 30 min at room temperature to blocking endogenous peroxidases. The slides were blocked with 1X Blocker™ BSA in TBS for 2 h at room temperature. The mouse-anti-human primary antibody for Ki-67 (1:400; cat. no. 9449; Cell Signaling Technology, Inc.) was added to the slides, which were incubated overnight at 4℃. Then, biotinylated goat-anti-mouse IgG secondary antibodies (1:500; cat. no. 14709; Cell Signaling Technology, Inc.) was added and incubated for 30 min at room temperature. HRP-conjugated streptavidin was used to attach peroxidase to biotinylated antibodies, and DAB chromogen was used for visualization. Then, hematoxylin was used to nuclear counterstain for 3.5 min at room temperature. The stained slides were observed under a FluoView FV1000 microscope (magnification, x200; Olympus Corporation), and 10 random fields per sample were captured. FV10-ASW Viewer (version 4.2; Olympus Corporation) was used to analyze images.

Luciferase assay. A375 and SK-MEL-28 cells were seeded in a 96-well plate at 70% confluence. The 3'-untranslated region (UTR) of Linc00961 containing miR-367-binding sites was

cloned into a pmirGLO dual-luciferase miRNA target expression vector (Promega Corporation), yielding pmirGLO-wild type (WT)-Linc00961. Mutations were introduced into potential miR-367-binding sites of Linc00961 using a QuikChange™ site-directed mutagenesis kit (Stratagene; Agilent Technologies, Inc.) to construct pmirGLO-mutant (MUT)-Linc00961. Subsequently, 20 nM miR-367 NC or mimics and 50 ng pmirGLO-WT/MUT-Linc00961 were co-transfected into $1x10^5$ A375 or SK-MEL-28 cells using Lipofectamine 2000 in 96 well plate. Cells were collected 48 h after transfection, and the relative firefly luciferase activities were measured using a dual-luciferase reporter assay system according to the manufacturer's protocol (Promega Corporation). *Renilla* luciferase activity served as an internal control.

RNA pull-down assay. The procedures for RNA pull-down assay was performed as described in our previous study (19). Briefly, full length Linc00961 and Linc00961-MUT transcripts were transcribed from pmirGLO-WT-Linc00961 and pmirGLO-MUT-Linc00961 *in vitro*. The restriction enzyme *Bam*HI was used to linearize the plasmids. Then, Ribo™ RNA max-T7 RNA polymerase and Biotin RNA Labeling kit (cat. no. C11002-1; Guangzhou RiboBio Co., Ltd.) was used to produce biotin-labeled RNAs, according to the manufacturer's instructions. Subsequently, 5 μg biotin-labeled Linc00961 or Linc00961-MUT was incubated with 1 mg cell lysates, which were lysed using NP40 solution (cat. no. P0013F; Beyotime Institute of Biotechnology) at 4˚C for 4 h. A negative control biotinylated probe was also included in the Biotin Labeling kit. Subsequently, the RNAs with biotin-labelled Linc00961 or Linc00961-MUT were mixed with 40 μl Dynabeads® MyOne™ Streptavidin C1 beads (cat. no. 65002; Invitrogen; Thermo Fisher Scientific, Inc.) and incubated on a rotator at 4˚C overnight. Subsequently, the pulled-down RNA was identified via RT-qPCR analysis, performed as previously described.

Statistical analysis. IBM SPSS statistical software (version 22.0) was used to perform statistical analysis. The experiments were repeated three times, and data were presented as the mean ± standard deviation. Student's t-test (for analysis of groups) and one-way ANOVA followed by least significant difference testing (for analysis of multiple groups) were used for data analysis. Kaplan-Meier curve and log-rank tests were used to analyze the survival rates of different groups. Pearson's correlation analysis was used to analyze the correlations between Linc00961 and miR-367 expression in patient with SM. P<0.05 was considered to indicate a statistically significant difference.

Results

Linc00961 is downregulated in tissues and cells of SM. RT-qPCR analysis indicated that Linc00961 was significantly downregulated in the tissues of 13 patients with SM compared with 13 patients with BN (P<0.05; Fig. 1A). Furthermore, analysis of the GSM3071633 dataset also revealed decreased expression levels of Linc00961 in SM tissues compared with BN tissues (P<0.05; Fig. 1B). In addition, Linc00961 levels were also significantly downregulated in SM cells

(A375, A2058 and SK-MEL-28) compared with the human epidermal melanocyte cell line, HEMa-LP (P<0.05; Fig. 1C). Subsequently, the prognostic value of Linc00961 expression levels for SM was investigated by analyzing TCGA data. It was revealed that the overall survival of patients with SM exhibiting high Linc00961 levels was significantly higher compared with those with low Linc00961 levels (Fig. 1D). These results indicated that Linc00961 was a potential tumor suppressor in SM. Therefore, in a subsequent experiment, the Linc00961 levels in A375 and SK-MEL-28 cells were upregulated using Lv-Linc00961 (P<0.05; Fig. S1A), and the effects of Linc00961 on the proliferation and invasion of A375 and SK-MEL-28 cells were further investigated.

Effects of Linc00961 on the proliferation and apoptosis of A375 and SK-MEL-28 cells in vitro. A CCK-8 assay revealed that the proliferation rates of A375 and SK-MEL-28 cells transfected with Lv-Linc00961 were significantly reduced compared with those of cells transfected with Lv-control (P<0.05; Fig. 2A and B). FCM assays indicated that the early apoptosis of A375 and SK-MEL-28 cells transfected with Lv-Linc00961 was promoted compared with in cells transfected with Lv-control (P<0.05; Fig. 2C and D).

Effects of Linc00961 on tumor growth and apoptosis of nude mice bearing A375 cells in vivo. Subsequently, the effects of Linc00961 on tumor growth in nude mice injected with A375 cells were determined. As shown by the growth curves, slower tumor growth and smaller tumor volumes were observed in the mice injected with A375 cells transfected with Lv-Linc00961 compared with Lv-control (P<0.05; Fig. 2E and F). Furthermore, Ki-67 assays revealed that the percentage of Ki-67 positive cells was significantly downregulated in mice injected with A375 cells transfected with Lv-Linc00961 (P<0.05; Fig. 3A and B). However, TUNEL assays revealed a more intense fluorescence signal indicative of apoptosis in the tissues of mice injected with A375 cells transfected with Lv-Linc00961 (P<0.05; Fig. 3C and D).

Effects of Linc00961 on the migration and invasion of A375 and SK-MEL-28 cells in vitro. The effects of Linc00961 on the migration and invasion of A375 and SK-MEL-28 cells were further explored. Cell migration assays revealed that the numbers of migrating A375 and SK-MEL-28 cells transfected with Lv-Linc00961 were reduced compared with cells transfected with Lv-control (P<0.05; Fig. 4A and B). Cell invasion assays demonstrated that the numbers of invasive A375 and SK-MEL-28 cells transfected with Lv-Linc00961 were also decreased compared with cells transfected with Lv-control (P<0.05; Fig. 4C and D).

Linc00961 is inversely correlated with miR-367 in SM. To explore the underlying mechanisms of Linc00961 in SM cells, miR-26a, miR-107, miR-367 and miR-5581 were identified as potential targeting miRNAs containing putative binding sites for Linc00961 via a search of an online bioinformatics database (miRDB). Subsequently, the expression levels of miR-367 were revealed to be significantly downregulated following the upregulation of Linc00961 expression in A375 (P<0.05; Fig. 5A) and SK-MEL-28 cells (P<0.05; Fig. 5B). However, the
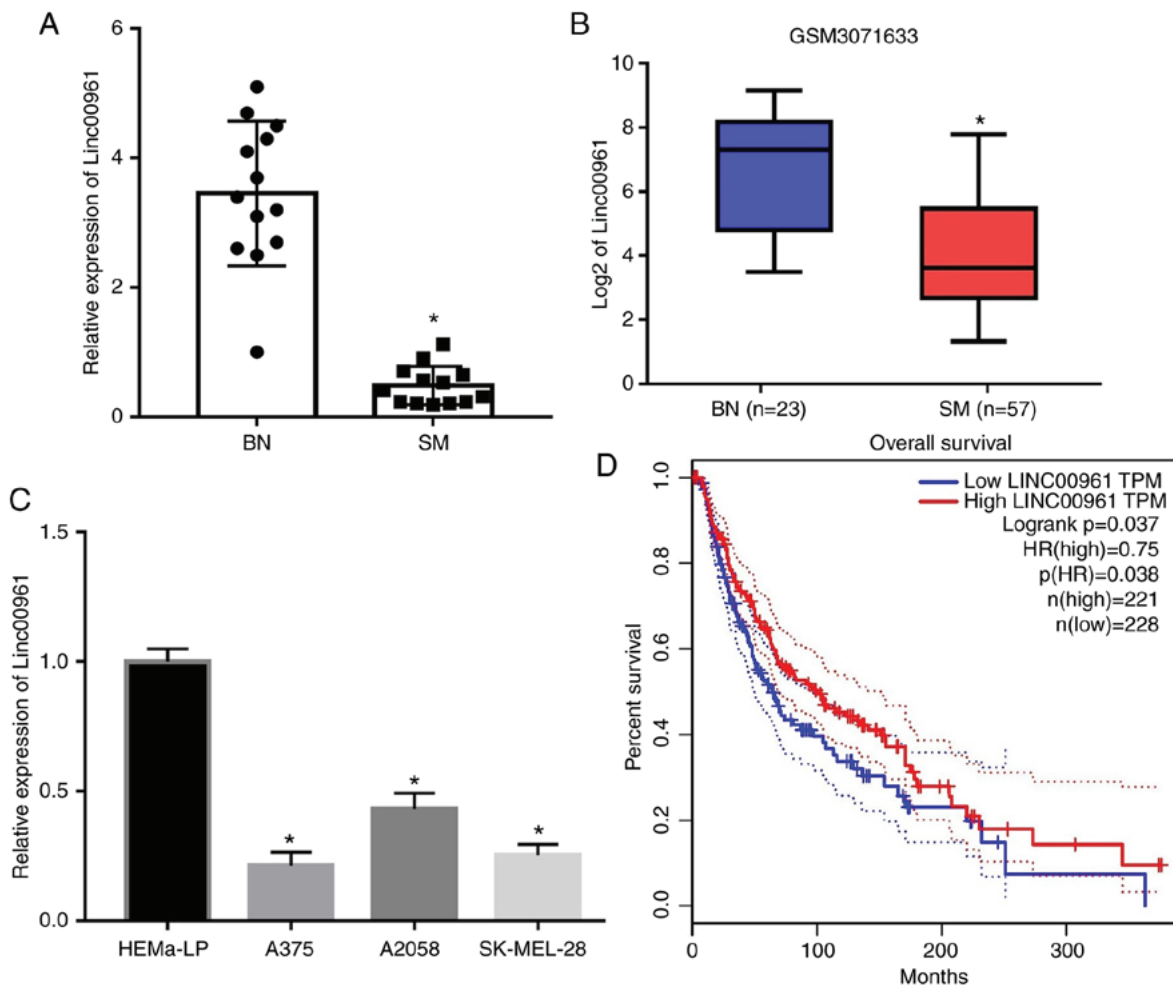
Figure 1. Linc00961 is downregulated in SM cells and the tissues of patients with SM. (A) Expression of Linc00961 in tissues of SM and BN. (B) Patients with SM in GSM3071633 exhibited decreased expression of Linc00961 compared with patients with BN. (C) Relative expression levels of Linc00961 in human epidermal melanocytes and SM cells. (D) Association of Linc00961 expression with the overall survival of SM patients. The Cancer Genome Atlas data were analyzed using the Gene Expression Profiling Interactive Analysis website. Data from three experiments are presented as mean ± SD. *P<0.05 vs. BN or HEMa-LP. Linc00961, long intergenic noncoding RNA 00961; SM, skin melanoma; BN, benign nevi; HR, hazard ratio.

expression levels of miR-26a, miR-107 and miR-5581 were not significantly altered following overexpression of Linc00961 in A375 (P>0.05; Fig. 5A) or SK-MEL-28 (P>0.05; Fig. 5B) cells. The results from RT-qPCR analysis revealed that miR-367 levels were upregulated in SM tissues (P<0.05; Fig. 5C), which were inversely correlated with Linc00961 levels (r=-0.394; P<0.05; Fig. 5D). Furthermore, miR-367 expression was also enhanced in SM cells (A375, A2058 and SK-MEL-28) compared with normal melanocytes (P<0.05; Fig. 5E).

Linc00961 directly binds with miR-367 in SM cells. To confirm whether Linc00961 could function as a ceRNA to competitively bind with miR-367, FISH was performed to identify the subcellular localization of Linc00961 in SK-MEL-28 cells. Linc00961 was revealed to be mainly expressed in cytoplasm and the nuclei (Fig. S2), indicating that Linc00961 could both function as a ceRNA and bind with RNA-binding proteins in SM cells. Subsequently, WT-Linc00961 and MUT-Linc00961 vectors were constructed to further explore the association between Linc00961 and miR-367 in SM (Fig. 5F). First, it was revealed that miR-367 expression levels were downregulated in A375 and SK-MEL-28 cells transfected with Lv-Linc00961

compared with A375 cells and SK-MEL-28 cells transfected with Lv-control (P<0.05; Fig. 6A). Dual-luciferase reporter assays indicated that the relative luciferase activities in A375 (P<0.05; Fig. 6B) and SK-MEL-28 cells (P<0.05; Fig. 6C) co-transfected with Linc00961-WT and miR-367 mimics were significantly decreased compared with cells transfected with miR-367 NC. By contrast, co-transfecting Linc00961-MUT and miR-367 mimics into A375 (P>0.05; Fig. 6B) and SK-MEL-28 cells (P>0.05; Fig. 6C) did not significantly affect the relative luciferase activity. Furthermore, biotin-labeled RNA pulldown assays demonstrated that a bio-Linc00961 probe could directly pull down miR-367, but the associated bio-Linc00961-MUT-probe failed to pull down miR-367 in A375 (P<0.05; Fig. 6D and E) or SK-MEL-28 cells (P<0.05; Fig. 6D and F). Collectively, these results indicated that Linc00961 could directly sponge miR-367 at special recognition sites in SM cells.

Linc00961 functions as a ceRNA to inhibit the proliferation and invasion of A375 and SK-MEL-28 cells by directly sponging miR-367. To investigate whether Linc00961 inhibited the malignant behaviors of A375 and SK-MEL-28 cells via
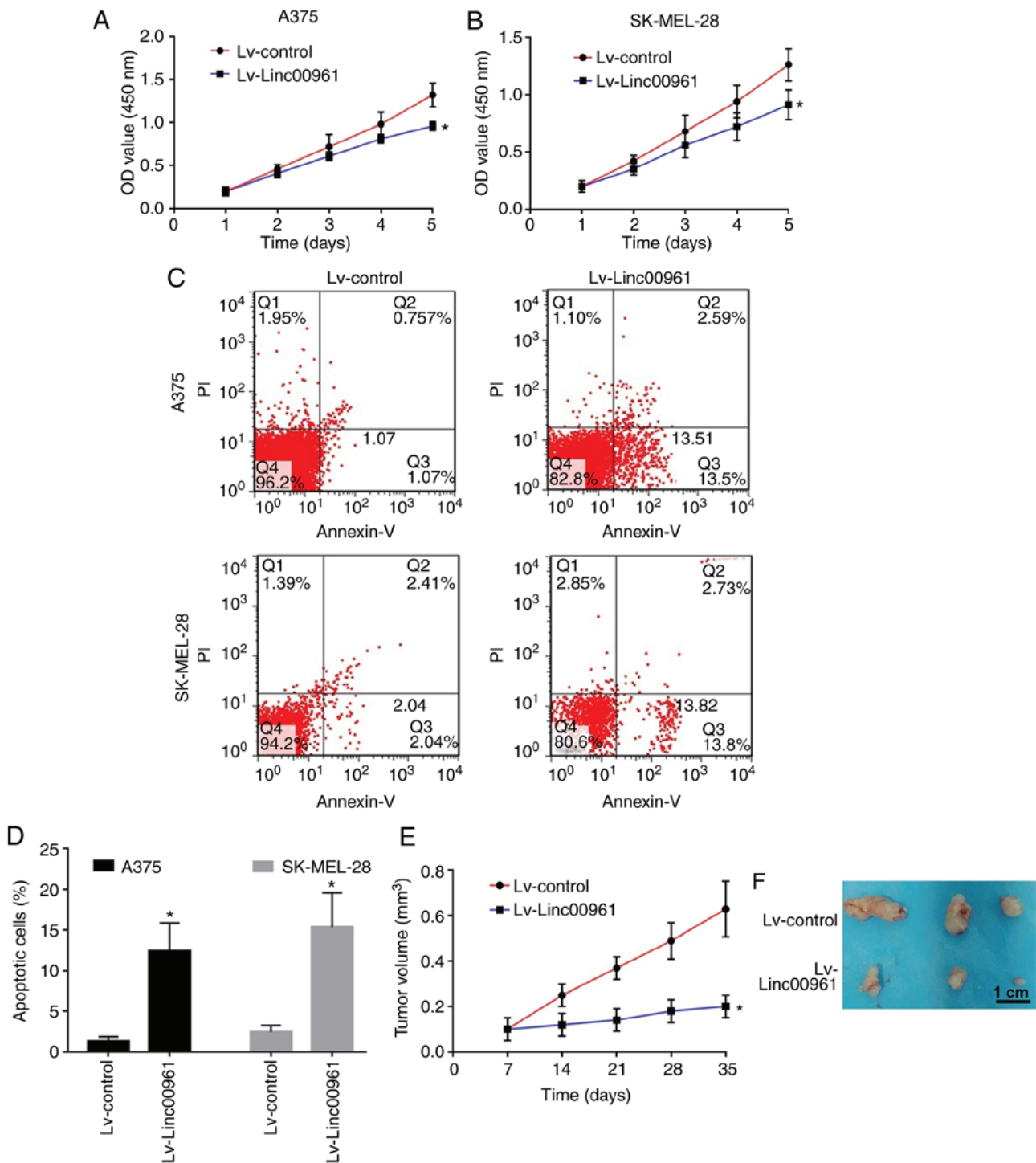
Figure 2. Effects of Linc00961 on the proliferation and apoptosis of A375 and SK-MEL-28 cells. Effects of Linc00961 on the proliferation of (A) A375 and (B) SK-MEL-28 cells, as determined using a Cell Counting Kit-8 assay. (C) Effects of Linc00961 on the apoptosis of A375 and SK-MEL-28 cells, detected via flow cytometry. (D) Statistical analysis of the early apoptotic rates of A375 and SK-MEL-28 cells infected with Lv-control and Lv-Linc00961. (E) Tumor growth curve of A375 cells transfected with Lv-control and Lv-Linc00961. (F) Digital pictures of the resected tumors of animals injected with A375 cells infected with Lv-control (n=3) and Lv-Linc00961 (n=3), captured after 35 days. The maximum diameters of Lv-control and Lv-Linc00961 were 1.718 and 0.737 cm, respectively. Scale bar=1 cm. Data from three experiments are presented as the mean ± SD. *$P<0.05$ vs. Lv-control. Linc00961, long intergenic noncoding RNA 00961; Lv, lentivirus; PI, propidium iodide.

binding to miR-367, which was established as an oncogenic miRNA in SM (21), the combined effects of overexpression of both Linc00961 and miR-367 on proliferation and invasion of A375 and SK-MEL-28 cells were examined. miR-367 mimics were transfected into A375 and SK-MEL-28 cells in order to upregulate miR-367 expression (P<0.05; Fig. S1B).

Subsequently, it was confirmed that the decreased miR-367 expression level resulted from Linc00961 overexpression, and that recovery of the expression of miR-367 was identified following co-transfection with miR-367 mimics (Fig. 7A). Subsequently, CCK-8 and FCM assays were employed to investigate the effects of Lv-Linc00961 on the proliferation and
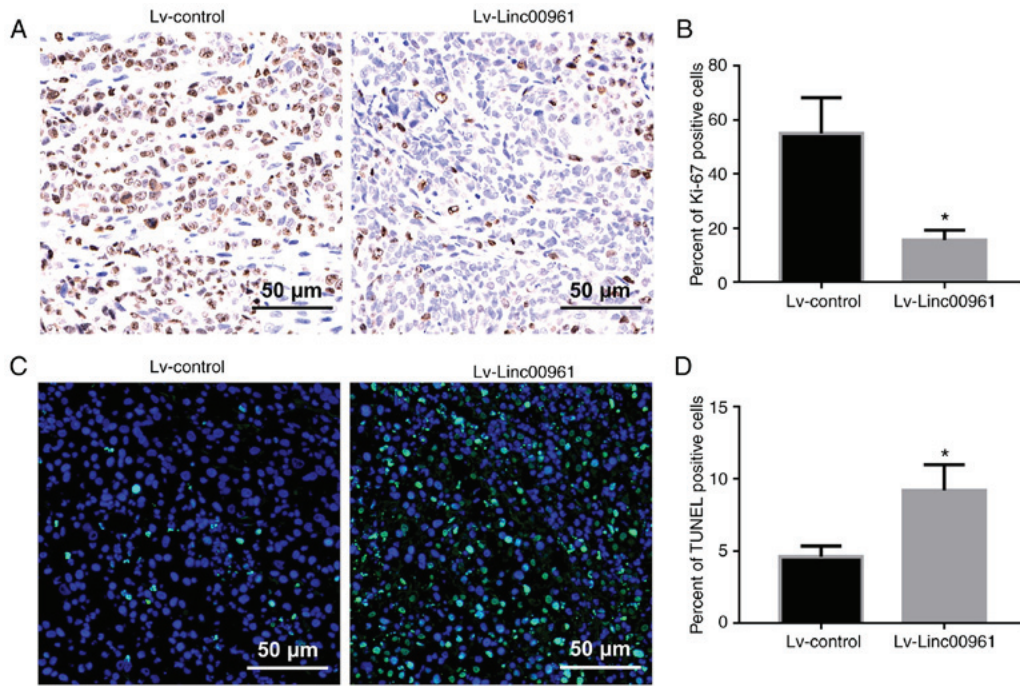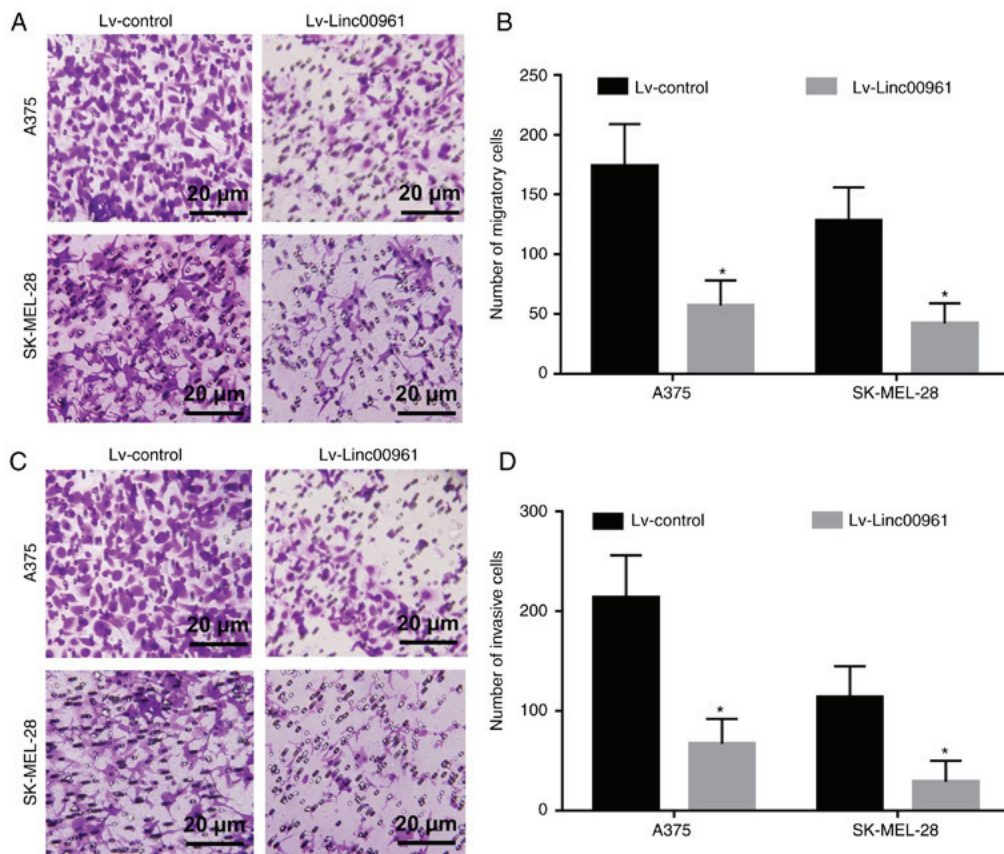
Figure 3. Effects of Linc00961 on proliferation and apoptosis in tumors from nude mice injected with A375 cells. (A) Ki-67 positive cells in nude mice bearing A375 cells transfected with Lv-control and Lv-Linc00961. (B) Statistical analysis of the percentage of Ki-67 positive cells in xenograft tumors. (C) TUNEL-positive cells in nude mice bearing A375 cells transfected with Lv-control and Lv-Linc00961. (D) Statistical analysis of the percentage of TUNEL-positive cells in xenograft tumors. Scale bar=50 μm. Data from three experiments are presented as the mean ± SD. *P<0.05 vs. Lv-control. Linc00961, long intergenic noncoding RNA 00961; Lv, lentivirus.

Figure 4. Effects of Linc00961 on the migration and invasion of SM cells. (A) Effects of Linc00961 on the migration of A375 and SK-MEL-28 cells, as determined by a Transwell assay. (B) Statistical analysis of the numbers of migratory A375 and SK-MEL-228 cells. (C) Effects of Linc00961 on cell invasion of A375 and SK-MEL-28 cells, as determined by a Matrigel-coated Transwell assay. (D) Statistical analysis of the numbers of invasive A375 and SK-MEL-228 cells. Scale bar=20 μm. Data from three experiments are presented as the mean ± SD. *P<0.05 vs. Lv-control. LINC00961, long intergenic noncoding RNA 00961; Lv, lentivirus.
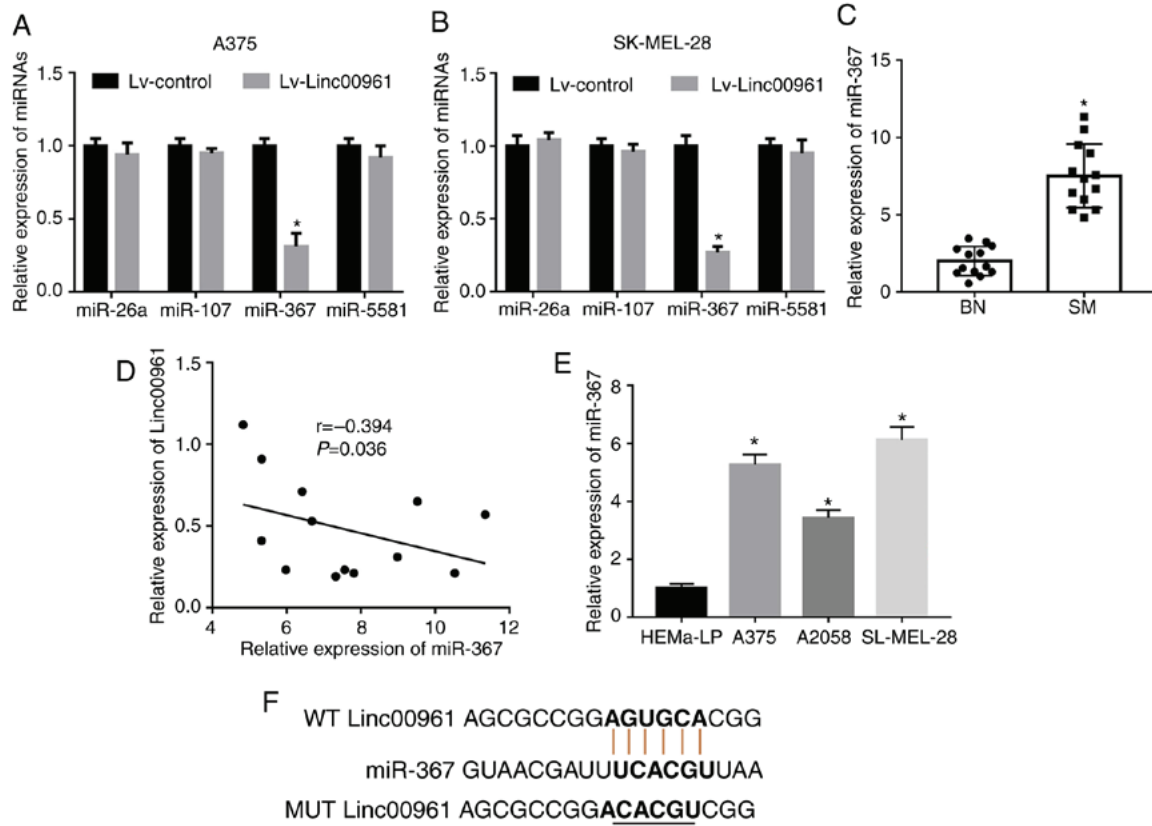
Figure 5. Linc00961 expression is inversely correlated with miR-367 expression in SM. Effects of Linc00961 on the expression of miRNAs that possessed putative binding sites for Linc00961 in (A) A375 and (B) SK-MEL-28 cells. (C) Expression levels of miR-367 in SM and BN tissues. (D) Association between miR-367 and Linc00961 in SM tissues. (E) Expression levels of miR-367 in SM cells and human epidermal melanocytes. (F) WT and MUT targeting regions of Linc00961 for miR-367. Data from three experiments are presented as the mean ± SD. $^{*}P<0.05$ vs. control (Lv-control, BN, HEMa-LP). Linc00961, long intergenic noncoding RNA 00961; miR, microRNA; SM, skin melanoma; BN, benign nevi; WT, wild-type; MUT, mutant.

apoptosis of A375 and SK-MEL-28 cells, and these inhibitory effects were rescued by co-transfection of miR-367 mimics ($P<0.05$; Fig. 7B-E). Similarly, Transwell assays demonstrated that up-regulation of miR-367 could reverse the inhibitory effects of Lv-Linc00961 on cell migration and invasion of A375 and SK-MEL-28 cells ($P<0.05$; Fig. 8A-D).

Silencing PTEN ameliorates the inhibitory effects of Linc00961 on proliferation and invasion of SM cells. Previous studies had indicated that PTEN was a direct target of miR-367 in SM cells (21,22). Thus, it was hypothesized that the inhibitory effects of Linc00961 in SM may be mediated via PTEN. To investigate this, the effects of Linc00961 on the mRNA and protein expression levels of PTEN were examined, and both were revealed to be upregulated as a consequence of Linc00961 overexpression, although the mRNA and protein expression levels were subsequently decreased following co-transfection of miR-367 mimics (Fig. 9A and B). In functional terms, the proliferation, migration and invasion of A375 and SK-MEL-28 cells infected with Lv-Linc000961 were restored following the silencing of PTEN (Fig. S1C); the effects on proliferation are presented in Fig. 9C and D, whereas those on migration and invasion are presented in Figs. S3, and 9F and G. Furthermore, PTEN knockdown rescued the increase in apoptosis induced by Linc00961 overexpression in A375 and SK-MEL-28 cells (Figs. 9E and S4). Collectively, these results indicated that

Linc00961 inhibited the proliferation and invasion of A375 and SK-MEL-28 cells by targeting the miR-367/PTEN axis.

Discussion

LncRNAs have been identified as crucial regulators and biomarkers in SM (13,23). In the present study, it was revealed that Linc00961 was upregulated in SM tissues and cells compared with BN tissues and human epidermal melanocytes. In addition, Linc00961 expression was demonstrated to be positively associated with the 5-year overall survival rate of patients with SM by analyzing TCGA data; however, in the present study, as only 13 SM tissues were collected, the sample size was too small to analyze associations between Linc00961 expression and the clinicopathological features of melanoma patients. Additionally, Linc00961 overexpression inhibited the proliferation, migration and invasion, and promote the apoptosis of SM cells *in vitro*. Furthermore, to the best of our knowledge, the first evidence was provided that Linc00961 is able to sponge miR-367 and upregulate the expression of PTEN, a direct target of miR-367 in SM (21,22). Additionally, restoration of miR-367 or silencing of PTEN expression reversed the inhibitory effects of Linc00961 overexpression on SM cells. Collectively, these results indicated that Linc00961 may function as a ceRNA to inhibit cell proliferation and invasion in SM cells by targeting the miR-367/PTEN axis (Fig. 10).
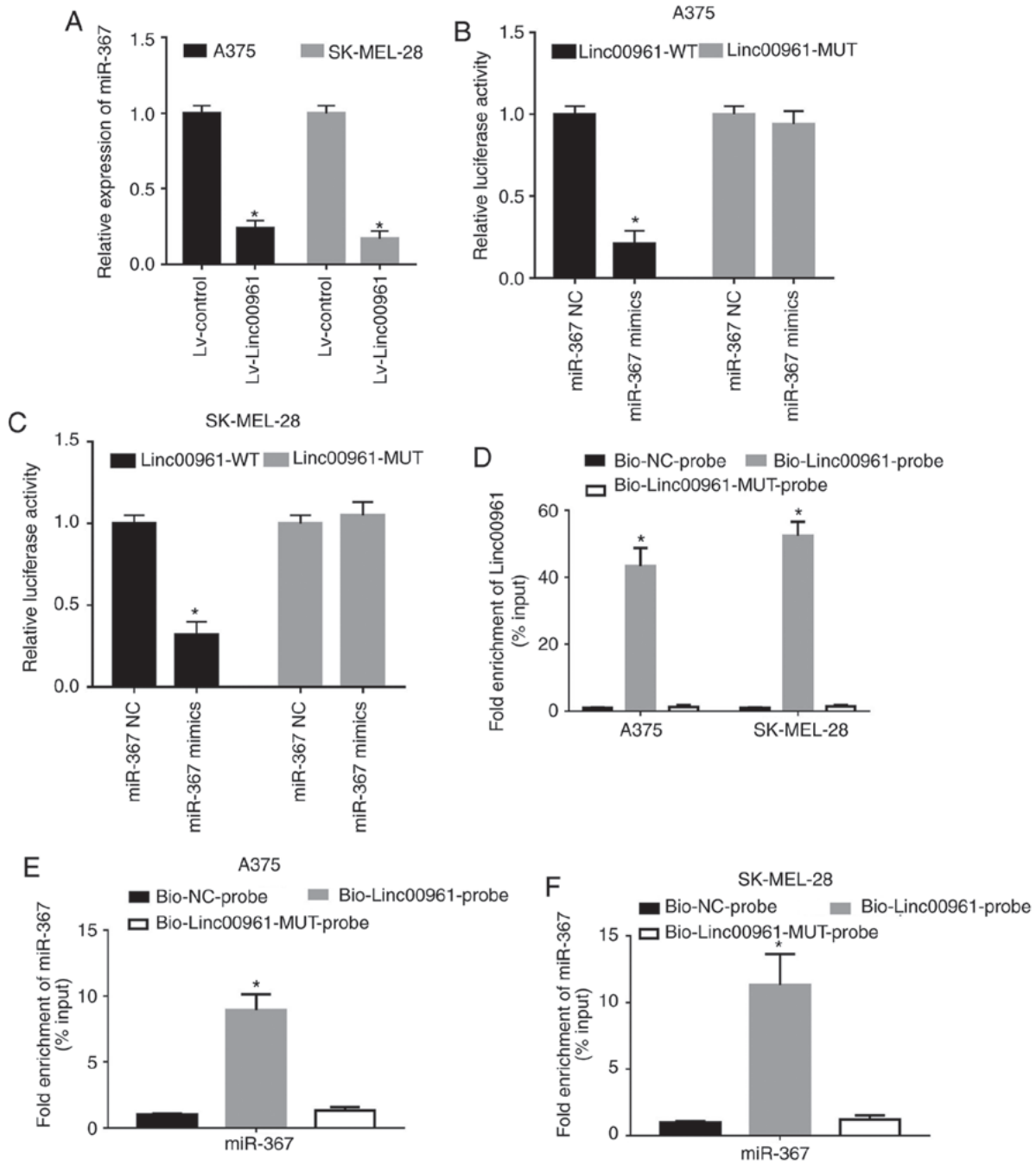
Figure 6. Linc00961 directly sponges miR-367 in SM cells. (A) Effects of Linc00961 on the expression of miR-367 in SM cells. Relative luciferase activity in (B) A375 and (C) SK-MEL-28 cells co-transfected with Linc00961-WT or LINC00961-MUT luciferase plasmid and miR-367 NC or mimics. (D) Detection of LINC00961 in RNA pulled down by Bio-Linc00961, Bio-Linc00961-MUT or Bio-NC probes. Detection of miR-367 in RNA pulled down by Bio-Linc00961, Bio-Linc00961-MUT or Bio-NC probes in (E) A375 and (F) SK-MEL-28 cells. Data from three experiments are presented as the mean ± SD. *P<0.05 vs. control (Lv-control, miR-367 NC, Bio-NC-probe). Linc00961, long intergenic noncoding RNA 00961; miR, microRNA; SM, skin melanoma; NC, negative control; WT, wild-type; MUT, mutant; Bio, biotinylated.

A recently published study reported that Linc00961 encoded a novel polypeptide termed SPAAR, which is involved in mTOR complex 1 activation and muscle regeneration (14,24). Additionally, the expression profile and potential function of Linc00961 in genesis and progression of human cancers was preliminarily established; Linc00961 was shown to suppress the invasion and migration of NSCLC cells *in vitro*, and metastasis *in vivo* (25). Furthermore, Linc00961 was also reported to inhibit cell proliferation and promote cell apoptosis by upregulating the levels of proliferating cell nuclear antigen and suppressing the expression of Bax protein in NSCLC (17). Furthermore, Linc00961 was also downregulated in lung squamous cell carcinoma and demonstrated to be a capable diagnostic biomarker (26). In glioma, Linc00961 was revealed to be downregulated in tissues and cell lines, and its expression was inversely associated with pathological features, poor overall survival and unfavorable prognosis (16), indicating that Linc00961 functions as a tumor suppressor in glioma. In renal cell carcinoma (RCC), it was revealed that Linc00961 suppressed RCC progression by inhibiting the
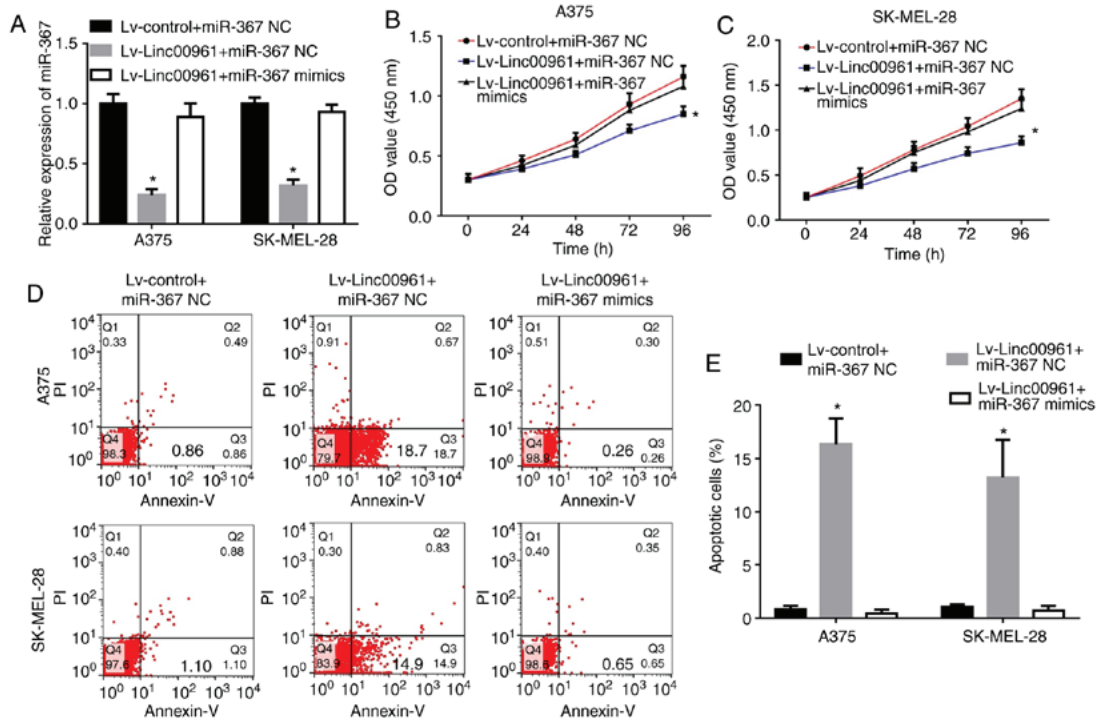
Figure 7. Upregulation of miR-367 reverses the effects of Linc00961 on the proliferation and apoptosis of skin melanoma cells. (A) Expression of miR-367 in A375 and SK-MEL-28 cells transfected with Lv-control + miR-367 NC, Lv-Linc00961 + miR-367 NC or Lv-Linc00961 + miR-367 mimics, as determined via reverse transcription-quantitative PCR. Proliferation of (B) A375 and (C) SK-MEL-28 cells transfected with Lv-control + miR-367 NC, Lv-Linc00961 + miR-367 NC or Lv-Linc00961 + miR-367 mimics, as determined by a Cell Counting Kit-8 assay. (D) Apoptosis of A375 and SK-MEL-28 cells transfected with Lv-control + miR-367 NC, Lv-Linc00961 + miR-367 NC or Lv-Linc00961 + miR-367 mimics, as determined via flow cytometry. (E) Statistical analysis of early apoptotic rates of A375 and SK-MEL-228 cells transfected with Lv-control + miR-367 NC, Lv-Linc00961 + miR-367 NC or Lv-Linc00961 + miR-367 mimics. Data from three experiments are presented as the mean ± SD. *P<0.05 vs. Lv-control + miR-367 NC. Linc00961, long intergenic noncoding RNA 00961; Lv, lentivirus; miR, microRNA; NC, negative control; PI, propidium iodide.
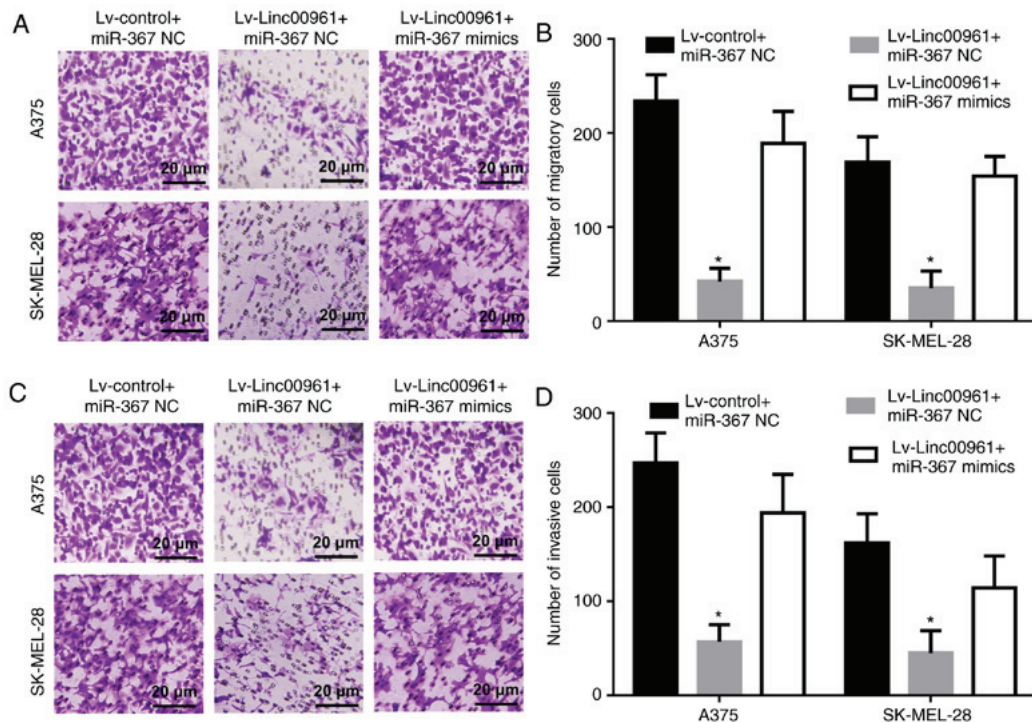

Figure 8. Upregulation of miR-367 reverses the effects of Linc00961 on the migration and invasion of SM cells. (A) Numbers of migratory A375 and SK-MEL-28 cells transfected with Lv-control + miR-367 NC, Lv-Linc00961 + miR-367 NC or Lv-Linc00961 + miR-367 mimics, determined by a Transwell assay. (B) Statistical analysis of the numbers of migratory A375 and SK-MEL-228 cells. (C) Numbers of invasive A375 and SK-MEL-28 cells transfected with Lv-control + miR-367 NC, Lv-Linc00961 + miR-367 NC or Lv-Linc00961 + miR-367 mimics, as determined by a Transwell assay. (D) Statistical analysis of the numbers of invasive A375 and SK-MEL-228 cells. Scale bar=20 μm. Data from three experiments are presented as the mean ± SD. *P<0.05 vs. Lv-control + miR-367 NC. Linc00961, long intergenic noncoding RNA 00961; Lv, lentivirus; miR, microRNA; NC, negative control.
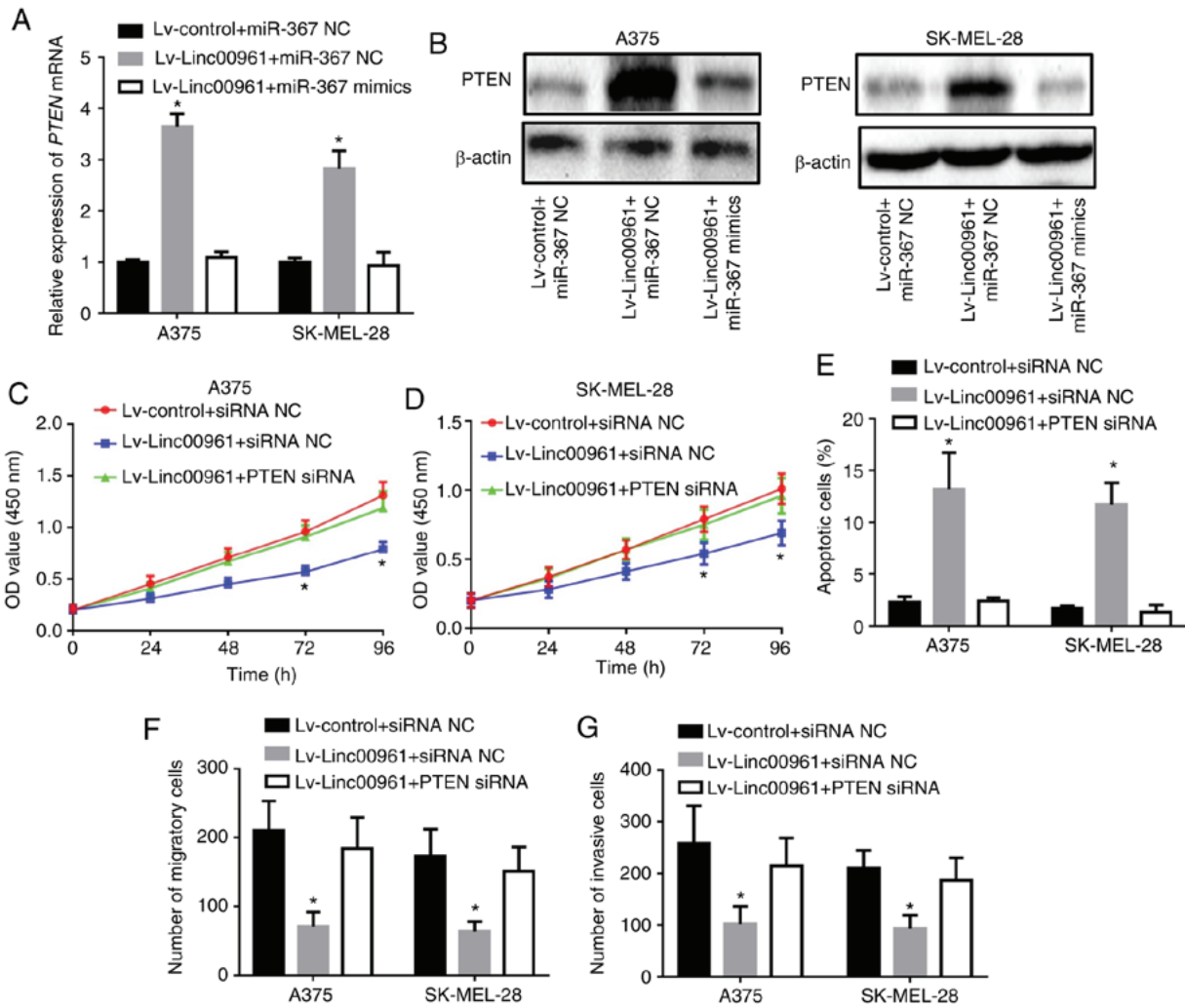
Figure 9. Silencing PTEN reverses the inhibitory effects of Linc00961 on the proliferation and invasion of SM cells. (A) mRNA and (B) protein expression of PTEN in A375 and SK MEL-28 cells transfected with Lv-control + miR-367 NC, Lv-Linc00961 + miR-367 NC or Lv-Linc00961 + miR-367 mimics. Proliferation of (C) A375 and (D) SK-MEL-28 cells transfected with Lv-control + siRNA NC, Lv-Linc00961 + siRNA NC or Lv-Linc00961 + PTEN siRNA, as determined by a Cell Counting Kit-8 assay. (E) Apoptosis of A375 and SK-MEL-28 cells transfected with Lv-control + siRNA NC, Lv-Linc00961 + siRNA NC or Lv-Linc00961 + PTEN siRNA, as determined via flow cytometry. Numbers of (F) migratory and (G) invasive A375 and SK-MEL-28 cells transfected with Lv-control + siRNA NC, Lv-Linc00961 + siRNA NC, or Lv-Linc00961 + PTEN siRNA, as determined via Transwell assays. Data from three experiments are presented as mean ± SD. $^*P<0.05$ vs. Lv-control + miR-367 NC or siRNA NC. Linc00961, long intergenic noncoding RNA 00961; PTEN, phosphate and tension homology deleted on chromosome 10; Lv, lentivirus; miR, microRNA; siRNA, small interfering RNA; NC, negative control.
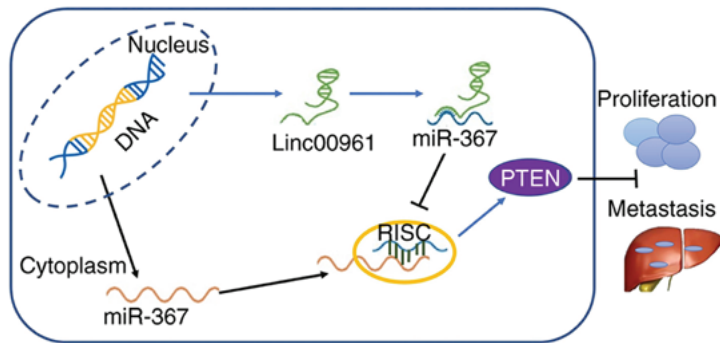

Figure 10. Mechanism underlying the regulatory functions of Linc00961 in skin melanoma. Linc00961 inhibits the proliferation and invasion of SM cells by targeting the miR-367/PTEN axis. Linc00961, long intergenic noncoding RNA 00961; miR-367, microRNA-367; PTEN, phosphate and tension homology deleted on chromosome 10; RISC, RNA-induced silencing complex.

epithelial-mesenchymal transition signaling pathway (27). Consistent with these previous studies, the present study also

demonstrated that Linc00961 functioned as a tumor suppressor gene in the carcinogenesis and development of SM. Linc00961

was demonstrated to inhibit the proliferation, and suppress the tumor growth of SM *in vitro* and *in vivo*. It also induced inhibitory effects on the migration and invasion of SM cells; however, the underlying mechanism of Linc00961's suppressive role in SM development is yet to be fully determined.

An increasing body of evidence has revealed that lncRNAs are able to function as ceRNAs to interfere with miRNAs and their downstream pathways. CeRNA regulatory networks have been demonstrated to be key regulators in autoimmune diseases and viral infections (28-30), and they are also commonly associated with carcinogenesis and the progression of different types of cancer (31-33), including gastric cancer and SM (34). For example, LncRNA HOTAIR promoted the tumorigenesis and progression of SM via the miR-152-3p/c-MET/PI3K/AKT pathway (35). LncRNA activated by TGF-β, acting as a ceRNA against miR-590-5p, promoted the proliferation and invasion of SM cells (19). In the present study, miR-367 was identified as a potential targeting miRNA that possessed putative binding sites for Linc00961. It was subsequently shown that Linc00961 could directly sponge and bind to miR-367 at special recognition sites. Thus, the role of miR-367 in Linc00961's suppressive role in SM was then investigated.

miR-367 has been revealed to be involved in the carcinogenesis and progression in multiple types of cancer, including NSCLC and glioma (36,37). It is associated with the role of oncogenic or tumor-suppressive genes, depending on the type of cancer involved. For example, miR-367 promoted tumor growth in NSCLC, was associated with an unfavorable prognosis, and stimulated Wnt cascade activation by directly targeting the gene, F-box and WD repeat domain containing 7 (36). Conversely, upregulation of miR-367 was associated with a favorable prognosis for patients with high-grade glioma (37). In the case of melanoma, miR-367 was shown to promote the proliferation and invasion of cutaneous SM (21) or uveal melanoma (22) by downregulating PTEN expression. In the present study, it was demonstrated that the suppressive effects of Linc00961 on malignant phenotypes of SM cells were rescued by miR-367 overexpression or PTEN knockdown. Therefore, combining the results observed in previous studies with our present findings supports the hypothesis that Linc00961 functions as a ceRNA to inhibit the proliferation and invasion of SM by targeting the miR-367/PTEN axis.

In conclusion, it was revealed that Linc00961 is a potential tumor suppressor in SM. Linc00961 could inhibit cell proliferation, and promote the apoptosis of SM cells *in vivo* and *in vitro*. Furthermore, Linc00961 also suppressed the migration and invasion of A375 and SK-MEL-28 cells. In investigating the underlying mechanism, the present study also demonstrated that Linc00961 functioned as a sponge of miR-367 to enhance PTEN expression, and that miR-367 overexpression or PTEN knockdown rescued the inhibitory effects of Linc00961 overexpression on A375 and SK-MEL-28 cells. The present study has provided novel insight into the regulatory mechanisms of Linc00961 and the miR-367/PTEN axis in SM, and may provide a novel target for the treatment of SM in the future.

Acknowledgements

Funding

Availability of data and materials

The datasets used and/or analyzed during the current study are available from the corresponding author on reasonable request.

Authors' contribution

LJW conceived and designed the experiments. XM, KHM, and RG performed the majority of the experiments. YZ and DH were involved in animal experiments, data analysis and compilation. LJW drafted the manuscript. All authors have read and approved the manuscript, and agree to be accountable for all aspects of the research in ensuring that the accuracy or integrity of any part of the work are appropriately investigated and resolved.

Ethics approval and consent to participate

All animal experiments were approved by the Animal Care and Use Committee of Xi'an Jiaotong University and performed in accordance with institutional guidelines. The human study was performed in accordance with the principles of the Declaration of Helsinki and approved by the Ethical Committee of the First Affiliated Hospital of Xi'an Jiaotong University. All the patients enrolled in the present study provided their informed consent for the use of their resected tissues in this research.

Patient consent for publication

Not applicable.

Competing interests

The authors declare that they have no competing interests.

References

1. Siegel RL, Miller KD and Jemal A: Cancer statistics, 2019. CA Cancer J Clin 69: 7-34, 2019.
2. Zhou J, Jin B, Jin Y, Liu Y and Pan J: The antihelminthic drug niclosamide effectively inhibits the malignant phenotypes of uveal melanoma in vitro and in vivo. Theranostics 7: 1447-1462, 2017.
3. Rozeman EA, Dekker TJA, Haanen J and Blank CU: Advanced melanoma: Current treatment options, biomarkers, and future perspectives. Am J Clin Dermatol 19: 303-317, 2018.
4. Guo W, Wang H, Yang Y, Guo S, Zhang W, Liu Y, Yi X, Ma J, Zhao T, Liu L, *et al*: Down-regulated miR-23a contributes to the metastasis of cutaneous melanoma by promoting autophagy. Theranostics 7: 2231-2249, 2017.
5. Huang Y: The novel regulatory role of lncRNA-miRNA-mRNA axis in cardiovascular diseases. J Cell Mol Med 22: 5768-5775, 2018.

6. Yu B and Wang S: Angio-LncRs: LncRNAs that regulate angiogenesis and vascular disease. Theranostics 8: 3654-3675, 2018.
7. Krause HM: New and prospective roles for lncRNAS in organelle formation and function. Trends Genet 34: 736-745, 2018.
8. Balas SM and Johnson AM: Exploring the mechanisms behind long noncoding RNAs and cancer. Noncoding RNA Res 3: 108-117, 2018.
9. Rafiee A, Riazi-Rad F, Havaskary M and Nuri F: Long noncoding RNAs: Regulation, function and cancer. Biotechnol Genet Eng Rev 34: 153-180, 2018.
10. Anastasiadou E, Faggioni A, Trivedi P and Slack FJ: The nefarious nexus of noncoding RNAs in cancer. Int J Mol Sci 19: pii: E2072, 2018.
11. Yu X, Zheng H, Tse G, Zhang L and Wu WKK: CASC2: An emerging tumour-suppressing long noncoding RNA in human cancers and melanoma. Cell Prolif 51: e12506, 2018.
12. Yu X, Zheng H, Tse G, Chan MT and Wu WK: Long non-coding RNAs in melanoma. Cell Prolif 51: e12457, 2018.
13. Richtig G, Ehall B, Richtig E, Aigelsreiter A, Gutschner T and Pichler M: Function and clinical implications of long non-coding RNAs in melanoma. Int J Mol Sci 18: pii: E715, 2017.
14. Matsumoto A, Pasut A, Matsumoto M, Yamashita R, Fung J, Monteleone E, Saghatelian A, Nakayama KI, Clohessy JG and Pandolfi PP: mTORC1 and muscle regeneration are regulated by the LINC00961-encoded SPAR polypeptide. Nature 541: 228-232, 2017.
15. Tajbakhsh S: lncRNA-encoded polypeptide SPAR(s) with mTORC1 to regulate skeletal muscle regeneration. Cell Stem Cell 20: 428-430, 2017.
16. Lu XW, Xu N, Zheng YG, Li QX and Shi JS: Increased expression of long noncoding RNA LINC00961 suppresses glioma metastasis and correlates with favorable prognosis. Eur Rev Med Pharmacol Sci 22: 4917-4924, 2018.
17. Huang Z, Lei W, Tan J and Hu HB: Long noncoding RNA LINC00961 inhibits cell proliferation and induces cell apoptosis in human non-small cell lung cancer. J Cell Biochem 119: 9072-9080, 2018.
18. Kunz M, Löffler-Wirth H, Dannemann M, Willscher E, Doose G, Kelso J, Kottek T, Nickel B, Hopp L, Landsberg J, et al: RNA-seq analysis identifies different transcriptomic types and developmental trajectories of primary melanomas. Oncogene 37: 6136-6151, 2018.
19. Mou K, Liu B, Ding M, Mu X, Han D, Zhou Y and Wang LJ: lncRNA-ATB functions as a competing endogenous RNA to promote YAP1 by sponging miR-590-5p in malignant melanoma. Int J Oncol 53: 1094-1104, 2018.
20. Livak KJ and Schmittgen TD: Analysis of relative gene expression data using real-time quantitative PCR and the 2(-Delta Delta C(T)) method. Methods 25: 402-408, 2001.
21. Long J, Luo J and Yin X: miR-367 enhances the proliferation and invasion of cutaneous malignant melanoma by regulating phosphatase and tensin homolog expression. Mol Med Rep 17: 6526-6532, 2018.
22. Ling JW, Lu PR, Zhang YB, Jiang S and Zhang ZC: miR-367 promotes uveal melanoma cell proliferation and migration by regulating PTEN. Genet Mol Res: 16: gmr16039067, 2017.
23. Liu XF, Hao JL, Xie T, Pant OP, Lu CB, Lu CW and Zhou DD: The BRAF activated non-coding RNA: A pivotal long non-coding RNA in human malignancies. Cell Prolif 51: e12449, 2018.
24. Rion N and Rüegg MA: LncRNA-encoded peptides: More than translational noise? Cell Res 27: 604-605, 2017.
25. Jiang B, Liu J, Zhang YH, Shen D, Liu S, Lin F, Su J, Lin QF, Yan S, Li Y, et al: Long noncoding RNA LINC00961 inhibits cell invasion and metastasis in human non-small cell lung cancer. Biomed Pharmacother 97: 1311-1318, 2018.
26. Chen WJ, Tang RX, He RQ, Li DY, Liang L, Zeng JH, Hu XH, Ma J, Li SK and Chen G: Clinical roles of the aberrantly expressed lncRNAs in lung squamous cell carcinoma: A study based on RNA-sequencing and microarray data mining. Oncotarget 8: 61282-61304, 2017.
27. Chen D, Zhu M, Su H, Chen J, Xu X and Cao C: LINC00961 restrains cancer progression via modulating epithelial-mesenchymal transition in renal cell carcinoma. J Cell Physiol 234: 7257-7265, 2019.
28. Li LJ, Zhao W, Tao SS, Leng RX, Fan YG, Pan HF and Ye DQ: Competitive endogenous RNA network: Potential implication for systemic lupus erythematosus. Expert Opin Ther Targets 21: 639-648, 2017.
29. Bossi L and Figueroa-Bossi N: Competing endogenous RNAs: A target-centric view of small RNA regulation in bacteria. Nat Rev Microbiol 14: 775-784, 2016.
30. Cai Y and Wan J: Competing endogenous RNA regulations in neurodegenerative disorders: Current challenges and emerging insights. Front Mol Neurosci 11: 370, 2018.
31. Yang C, Wu D, Gao L, Liu X, Jin Y, Wang D, Wang T and Li X: Competing endogenous RNA networks in human cancer: Hypothesis, validation, and perspectives. Oncotarget 7: 13479-13490, 2016.
32. Qu J, Li M, Zhong W and Hu C: Competing endogenous RNA in cancer: A new pattern of gene expression regulation. Int J Clin Exp Med 8: 17110-17116, 2015.
33. Guo LL, Song CH, Wang P, Dai LP, Zhang JY and Wang KJ: Competing endogenous RNA networks and gastric cancer. World J Gastroenterol 21: 11680-11687, 2015.
34. Sarkar D, Leung EY, Baguley BC, Finlay GJ and Askarian-Amiri ME: Epigenetic regulation in human melanoma: Past and future. Epigenetics 10: 103-121, 2015.
35. Luan W, Li R, Liu L, Ni X, Shi Y, Xia Y, Wang J, Lu F and Xu B: Long non-coding RNA HOTAIR acts as a competing endogenous RNA to promote malignant melanoma progression by sponging miR-152-3p. Oncotarget 8: 85401-85414, 2017.
36. Xiao G, Zhang B, Meng J, Wang J, Xu C, Tang SC, Li X, Zhang J, Liang R, Ren H and Sun X: miR-367 stimulates Wnt cascade activation through degrading FBXW7 in NSCLC stem cells. Cell Cycle 16: 2374-2385, 2017.
37. Guan Y, Chen L, Bao Y, Qiu B, Pang C, Cui R and Wang Y: High miR-196a and low miR-367 cooperatively correlate with unfavorable prognosis of high-grade glioma. Int J Clin Exp Pathol 8: 6576-6588, 2015.